Resource Allocation in Terrestrial-Satellite-Based Next Generation Multiple Access Networks With Interference Cooperation

Yaomin Zhang, Haijun Zhang, *Senior Member, IEEE*, Huan Zhou, *Member, IEEE*, Keping Long, *Senior Member, IEEE*, and George K. Karagiannidis, *Fellow, IEEE*

***Abstract*— In this paper, an uplink non-orthogonal multiple access (NOMA) terrestrial-satellite network is investigated, where the terrestrial base stations (BSs) communicate with satellite by backhaul link, and user equipments (UEs) share spectrum resource of access link. Firstly, a utility function which consists of the achieved terrestrial user rate and cross-tier interference caused by terrestrial BSs to satellite is design. Thus, the optimization problem can be modeled by maximizing the system utility function while satisfying the varying backhaul rate and UEs' quality of service (QoS) constraints. The optimization problem is highly non-convex and can not be solved directly. Thus, we decouple the original problem into user association sub-problem, bandwidth assignment sub-problem, and power allocation sub-problem. In user association sub-problem, an enhanced-caching, preference relation, and swapping based algorithm is proposed, where the satellite UEs are selected by the channel coefficient ratio. The terrestrial UEs association considers the both caching state and backhaul link. Then we derive the closed-form expression of the bandwidth assignment. In power allocation sub-problem, we convert the non-convex term of the target function into the convex one by the Taylor expansion, and solve the transformed convex problem by an iterative power allocation algorithm. Finally, a three-stages iterative resource allocation algorithm by joint considering the three sub-problems is proposed. Simulation results are discussed to show the effectiveness of the proposed algorithms.**

Manuscript received October 12, 2021; revised November 14, 2021; accepted December 17, 2021. Date of publication January 26, 2022; date of current version March 17, 2022. This work was supported in part by the National Key Research and Development Program of China under Grant 2020YFB1806103; in part by the Beijing Natural Science Foundation under Grant L212004; in part by the National Natural Science Foundation of China under Grant 62172255 and Grant 61872221; in part by the Fundamental Research Funds for the Central Universities under Grant FRFTP-19-002C1 and Grant RC1631; and in part by the Beijing Top Discipline for Artificial Intelligent Science and Engineering, University of Science and Technology Beijing. An earlier version of this paper was presented in part at the IEEE Global Communications Conference, Madrid, Spain, in 2021. *(Corresponding authors: Huan Zhou; Haijun Zhang.)*

Yaomin Zhang, Haijun Zhang, and Keping Long are with the Beijing Advanced Innovation Center for Materials Genome Engineering and the Beijing Engineering and Technology Research Center for Convergence Networks and Ubiquitous Services, Institute of Artificial Intelligence, University of Science and Technology Beijing, Beijing 100083, China (e-mail: yaominzhang@xs.ustb.edu.cn; haijunzhang@ieee.org; longkeping@ustb.edu.cn).

Huan Zhou is with the College of Computer and Information Technology, China Three Gorges University, Yichang 443002, China (e-mail: zhouhuan117@gmail.com).

George K. Karagiannidis is with the Department of Electrical and Computer Engineering, Aristotle University of Thessaloniki, 54 124 Thessaloniki, Greece (e-mail: geokarag@auth.gr).

Color versions of one or more figures in this article are available at https://doi.org/10.1109/JSAC.2022.3145810.

Digital Object Identifier 10.1109/JSAC.2022.3145810

***Index Terms*— Terrestrial-satellite networks, next generation multiple access, interference cooperation, power optimization, bandwidth allocation, matching.**

I. Introduction

THE integration of the satellite and terrestrial cell network has become a general trend for the future networks [1]–[4], which attracts attention of the academia and industry, recently. In terrestrial-satellite heterogeneous networks (HetNets), terrestrial base stations (BSs) provide high-rate communication link for user equipments (UEs), and the satellite network as the vital complement to the terrestrial radio networks, can provide global wide area coverage and high-capacity backhaul [5], [6]. The UEs can choose the access point (AP) depending on the different demands. However, there are still some challenges in terrestrial-satellite HetNets. For example, the scarce spectrum resource and high interference caused by the increasing number of users greatly affect the transmission efficiency of terrestrial-satellite HetNets [7]. Although orthogonal multiple access technology can avoid communication interference in terrestrial-satellite HetNets, the improvement of spectrum utilization and capacity is limited due to the fact that each orthogonal resource block can only serve one user in a time slot.

The non-orthogonal multiple access (NOMA) technology is recognized as an effective solution for rational and efficient utilization of spectrum resources, which has been considered to be the key part for next generation multiple access technology. With the NOMA technology, the same spectrum resource can be assigned to multiple users, which can bring obvious performance advantages over the traditional orthogonal access in some scenarios [8]–[10], especially in the wide coverage scenario by satellite communication. Integrating NOMA to terrestrial-satellite HetNets to improve communication performance and resource utilization tends to be an inevitable trend [11], [12]. Many scholars have developed lots of researches on the performance improvement of NOMA system [13]–[16]. The authors in [13] and [14] investigated the interference management problem of the NOMA based communication systems. The corresponding optimization algorithms were proposed to increase the sum rate of the NOMA systems. The authors in [15] focused on the study of distributed cluster allocation and power-bandwidth optimization scheme in the imperfect NOMA based downlink

HetNets, in which each BS can form clusters independently and determine the power-bandwidth allowance of each cluster distributively. Additionally, the paper [16] studied the energy efficiency maximization problem with power and bandwidth allocation in the NOMA network, where the authors derived the closed-form solution of bandwidth assignment and proposed an iterative algorithm with a generalized Dinkelbach style to achieve the power optimization.

Furthermore, the integration of NOMA and terrestrial-satellite system to fully utilize characteristics and advantages has been widely investigated [17]–[22]. The energy efficiency optimization in NOMA assisted terrestrial-satellite networks was investigated in [17]. The authors proposed an iterative UE association, subchannel, and power allocation method, which significantly improved system throughput. The paper [18] considered the beamforming optimization in the multibeam based NOMA satellite internet of things (IoT) networks. While [19] and [20] focused on the beamforming design and resource optimization for the NOMA terrestrial-satellite system. The authors of [21] studied the user association and power optimization problem, where the closed-form expression of the power solution was obtained and brought into the proposed user association scheme to obtain the global optimization solutions. Furthermore, the resource allocation problem in satellite based NOMA IoT networks was considered in [22], where the optimization problem was modeled as a Lyapunov framework and authors proposed a particle swarm algorithm to solve the joint optimization problem.

In addition, the wireless caching is a promising technology to reduce network load and achieve low-latency communication [23], [24]. By wireless caching, the popular content can be stored in the network edge nodes (BSs or UEs), i.e., the UEs can be served only via access link, that greatly releases the burden of backhaul link. The wireless caching technology can be applied in terrestrial-satellite HetNets to help improve system performance [25]–[27]. The backhaul link will be released with the aid of the wireless caching, which greatly reduces the service delay. The authors in [26] proposed to research resource management for computing, caching, and communication in terrestrial-satellite system, where both the network throughput fairness and data security can be guaranteed. The authors of [27] focused on the traffic offloading in the cache-enabled terrestrial-satellite networks, where the traffic offloading was achieved from the BSs through satellite's broadcast transmission. Furthermore, the co-existence of wireless caching and NOMA has been investigated in [13], [28]–[32]. The authors in [28] studied the energy efficient resource allocation problem in caching based NOMA network with terahertz communication, where the fronthual link was modeled by considering the influence of the caching. The deep learning network was considered to solve the optimization problem in caching enabled NOMA framework in [29] and [30]. And the authors of [31] proposed two NOMA-assisted wireless caching schemes to effectively decrease the latency for content delivery. Also the authors in [13] and [32] investigated the user association and power allocation in caching based NOMA networks, and solved it by the proposed joint algorithms.

Although there are lots of researches on resource allocation in wireless caching network, NOMA network, and terrestrial-satellite network, most papers were purely separated studies on NOMA terrestrial-satellite networks, caching based terrestrial-satellite networks, or caching based NOMA networks. The research of the caching based NOMA terrestrial-satellite networks, especially the resource allocation problem with the consideration of user association, power and bandwidth allocation has not been studied systematically. There are still some challenges in resource allocation of caching based NOMA terrestrial-satellite networks. Specifically, the effective resource allocation needs to guarantee both the reliable wireless backhaul transmissions and access network. And compared with the traditional terrestrial network, the interference in multicell NOMA terrestrial-satellite heterogeneous network is more complex, which also should be considered in the optimization problem. The above factors motivate this research.

In this paper, we investigated the uplink caching based NOMA terrestrial-satellite HetNets, where the terrestrial UEs and satellite UEs communicate with the same spectrum, and the satellite provides backhaul links for terrestrial BSs. Firstly, a utility function by the achieved rate of cellular UEs and cross-tier interference caused by BSs to satellite is constructed. Thus, the optimization problem is established by considering user access selection, backhaul constraint, and UE's QoS guarantee. Then, the optimization problem is decompose into AP-UE association, bandwidth assignment, and power allocation sub-problems. The corresponding algorithms are proposed to achieve the system optimization. Based on the conference version [33], we expansively consider the following points: (1) the detailed resource allocation process is presented now; (2) we discuss the time complexity for the proposed algorithms; (3) more simulation results are provided to verify the effectiveness of the proposed schemes. The contributions of this paper can be concluded as follows.

- We introduce an uplink caching based NOMA terrestrial-satellite heterogeneous network model, where the terrestrial UEs and satellite UEs use the same spectrum resources for communication. By the analysis of intra-cell interference, inter-cell interference, and cross-tier interference in the system model, the optimal successive interference cancellation (SIC) decoding order is derived. Then, a utility function which consists of the achieved rate of cellular UEs and cross-tier interference caused by BSs to satellite is constructed. By joint considering user association, backhaul constraint, and UE's QoS guarantee, the resource allocation problem for system utility maximization is modeled.
- The original optimization problem is highly non-convex and has NP complexity. Thus, we divide it into three stages and solve each sub-problem independently. In the first stage, an enhanced-caching, preference relation, and swapping based AP-UE association algorithm is proposed, where the satellite UEs are first selected by the channel coefficient ratio. For the terrestrial UEs association, the caching state and backhaul link are both considered. In the second stage, the closed-form expression of the bandwidth allocation is derived. In the last stage, the non-convex objective function is convert into

TABLE I
LIST OF MODEL NOTATION

$\mathbb{K}$, $\mathbb{U}$	Set of terrestrial BSs and UEs
K, U	Number of terrestrial BSs and UEs
M_k	Number of terrestrial cell k or satellite $L+1$
$\mathbb{X}$, $x_{u,k}$	User association matrix, association indicator of UE u to BS k or Satellite $K+1$
β	Bandwidth assignment coefficient
$\mathbb{P}$, $p_{u,k}$	Power allocation matrix, power of UE u to BS k or Satellite $K+1$
$h^B_{u,k}$, h^S_u	channel coefficients
$g^B_{u,k}$	Caching index of UE u to BS k
$I^{B,in}_{u,k}$	Interference of UE u to BS k from the same cell
$I^{B,out}_{u,k}$	Interference of UE u to BS k from the other cells
$I^{SB}_{u,k}$	Interference of UE u to BS k from the satellite UEs

the convex one by the successive convex approximation method, and then solve the sub-problem by an iterative power allocation algorithm.

- A three-stages iterative resource allocation algorithm is proposed to obtain the optimization solutions, and the corresponding algorithm is designed. Furthermore, we provide the brief analysis on computational complexity for the proposed optimization algorithms. Finally, the simulation results are discussed to show the convergence and effectiveness of the proposed algorithms.

The remaining part of this paper is organized in the following. In section II, we introduce an uplink caching based NOMA terrestrial-satellite network architecture and formulate the utility optimization problem. Section III divides the original optimization problem into AP-UE association, bandwidth assignment, and power allocation sub-problems, and gives the solutions by the proposed methods. Then, the resource optimization algorithms are designed in Section IV. Section V gives the discussion of the numerical simulation results. Finally, we conclude the paper in Section VI.

II. System Model and Problem Formulation

In this section, the caching based NOMA terrestrial-satellite HetNet model is briefly described. Then we construct the utility function and formulate the optimization problem by considering user association, bandwidth assignment, and power allocation. Some notations of this paper are shown in Table I.

A. System Model

We concentrate on the uplink communication scenario of the terrestrial-satellite network as shown in Fig. 1, where K BSs and one satellite are deployed to serve U terrestrial UEs. The BS and UE are denoted as $\mathbb{K} = \{1, \cdots, k, \cdots, K\}$ and $\mathbb{U} = \{1, \cdots, u, \cdots, U\}$, respectively. And the satellite is denoted as $K+1$. The total system bandwidth B is divided into two parts for the fronthaul link and backhaul link. For the fronthaul link, all the UEs share the $(1-\beta)B$ to communicate with the terrestrial BSs or satellite. For the backhaul link, all the BSs share the βB to communicate with the satellite. It is assumed that $U > K+1$. With the wireless caching technology, the

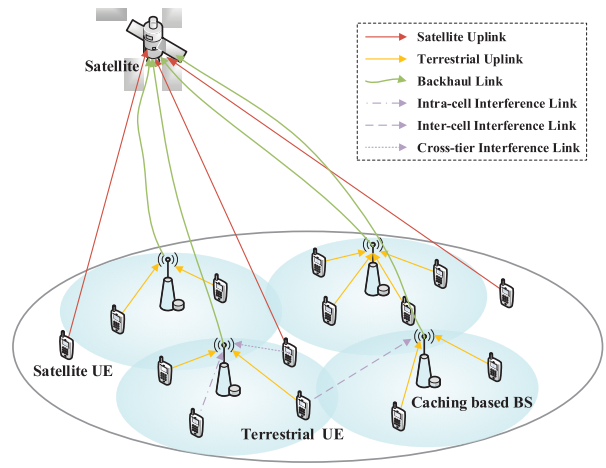

Fig. 1. The caching-based NOMA terrestrial-satellite network architecture.

BSs can store popular contents to achieve data offloading [34]. In the system model, NOMA technology is implemented for multiuser transmission. The terrestrial-satellite system links are supported by C-band transmission. Thus, the co-channel interference of terrestrial cellular UEs in terrestrial-satellite HetNets includes the successive interference caused by NOMA (intra-cell interference), terrestrial inter-cell interference, and cross-tier satellite interference. The detailed model analysis is presented in the following.

1) Terrestrial Communication Model: In the terrestrial networks, a BS can serve multiple UEs by NOMA. Let M_k be the UEs set served by BS k, thus the received signal of BS k from the UE u can be denoted as

$$\begin{aligned} y_{u,k} = {} & h^B_{u,k}\sqrt{p_{u,k}}s^B_{u,k} + h^B_{u,k}\sum_{j\in M_k\setminus\{u\}}\sqrt{p_{j,k}}s^B_{j,k} \\ & + \sum_{i\in\mathbb{K}\setminus\{k\}}\sum_{j\in M_i} h^B_{j,k}\sqrt{p_{j,i}}s^B_{j,i} \\ & + \sum_{j\in M_{K+1}} h^B_{j,k}\sqrt{p_{j,K+1}}s^S_j + \varsigma_k, \end{aligned} \tag{1}$$

where $p_{u,k}$ denotes the power of UE u to BS k or satellite $K+1$, $h^B_{u,k}$ is the corresponding channel coefficient of cellular UE u towards BS k, $s^B_{u,k}$ and $s^S_{j,K+1}$ are the transmission signal from UE u to BS k and UE j to satellite, respectively. The additive white Gaussian noise (AWGN) is considered with distribution of $\varsigma \sim CN(0, \sigma^2)$, where σ^2 is variance. Thus, the received signal-to-interference-plus-noise ratio (SINR) of BS k from terrestrial UE u is

$$\gamma^B_{u,k} = \frac{|h^B_{u,k}|^2 p_{u,k}}{I^{B,in}_{u,k} + I^{B,out}_{u,k} + I^{SB}_{u,k} + \sigma^2}, \tag{2}$$

where $I^{B,in}_{u,k} = |h^B_{u,k}|^2 \sum_{j\in M_k} p_{j,k}$, $I^{B,out}_{u,k} = \sum_{i\in\mathbb{K}\setminus\{k\}}\sum_{j\in M_i}|h^B_{j,k}|^2 p_{j,i}$, and $I^{SB}_{u,k} = \sum_{j\in M_{K+1}}|h^B_{j,k}|^2 p_{j,K+1}$ are the intra-cell interference, inter-cell interference, and cross-tier interference, respectively.

Let β denote the backhaul bandwidth allocation coefficient, and $\mathbb{X}[x_{u,k}]_{U\times K+1}$ denote the user association indicator, where $x_{u,k} = 1$ denotes that UE u is served by BS k, and $x_{u,k} = 0$, otherwise. Thus, The achieved transmission rate of

BS k from UE u can be obtained as

$$r_{u,k}^{B} = (1-\beta)B\log_2(1+\gamma_{u,k}^{B}), \tag{3}$$

and the achieved sum rate of cell k is

$$R_k^B = \sum_{u\in\mathbb{U}} x_{u,k} r_{u,k}^B. \tag{4}$$

2) Satellite Communication Model: Similarly, the received signal of the satellite from the UE u is

$$y_{u,K+1} = h_u^S\sqrt{p_{u,K+1}}s_u^S + h_u^S \sum_{j\in M_{K+1}} \sqrt{p_{j,K+1}}s_j^S + \sum_{i\in\mathbb{K}}\sum_{j\in M_i} h_j^S\sqrt{p_{j,i}}s_{j,i}^B + N_{K+1}, \tag{5}$$

where h_u^S denotes the channel coefficient of UE u towards satellite. The received SINR of the satellite from the satellite UE u is

$$\gamma_u^S = \frac{|h_u^S|^2 p_{u,K+1}}{\underbrace{|h_u^S|^2 \sum_{j\in M_{K+1}\setminus\{u\}} p_{j,K+1}}_{\text{intra-satellite interference}} + \underbrace{\sum_{i\in\mathbb{K}}\sum_{j\in M_i} |h_j^S|^2 p_{j,i}}_{\text{BS-satellite interference}} + \sigma^2}. \tag{6}$$

The interference of satellite UEs consists of intra-satellite interference and BS-satellite interference. Assume that satellite UEs communicate with a fixed transmission power. Thus, the received SINR of satellite is influenced by cross-tier interference caused by terrestrial UEs.

3) Caching Model: The local caching capability can realize traffic offloading and reduce network backhaul pressure. By wireless caching, the popular data can be cached in BSs at the edge of the network. The UEs can directly download the content from the local storage of BSs, instead of the core network through backhaul with limited capacity, thus reducing traffic overhead and communication time. Different caching strategy can influence the power allocation values. The caching index $\mathbb{G}[g_{u,k}]_{U\times K}$ is provided, where $g_{u,k}=1$ indicates BS k successfully caches the requested content of UE u during the caching phase (Assume the default cached content is the required content), and $g_{u,k}=0$, otherwise. In this paper, by the limitation of caching capability and the efficient use of cached content, the content required by each UE can be cached by at most one BS, and each BS is subject to the caching constraint of the maximum buffer capability. It is assumed that each BS has the same buffer capability. The mathematical expression is

$$\sum_{k\in} g_{u,k} \le 1, \quad \sum_{j\in\{M_k\}} g_{j,k} \le g^{\max}. \tag{7}$$

4) Backhaul Capacity: As shown in Fig. 1, the terrestrial UEs can request content to the satellite by BSs. The fronthaul link between terrestrial UEs and BSs is constrained by the backhaul link between BSs and satellite. Based on the caching strategy, when $g_{u,k}=1$, the BSs can provide services through cached content without sending request signaling to the superior, which reduces the link overhead and relieves backhaul pressure. The communication between BSs and satellite adopts orthogonal frequency division multiple access [35]. The backhaul SINR of the satellite from BS k is

$$\gamma_{k,s} = \frac{|h_{k,s}|^2 p_{k,s}}{|h_{k,s}|^2 \sum_{i\in\mathbb{K}\setminus\{k\}} p_{i,s} + \sigma^2}. \tag{8}$$

And the achieved backhaul rate of satellite at BS k is

$$R_{k,s} = \frac{|M_k| - \sum_{j\in M_k} g_{j,k}}{|M_k|}\frac{\beta B}{K}\log_2(1+\gamma_{k,s}), \tag{9}$$

where $|M_k| = \sum_{j\in\mathbb{U}} x_{j,k}$. The achieved backhaul sum rate is

$$R_s = \sum_{k\in\mathbb{K}} R_{k,s}. \tag{10}$$

5) SIC Decoding Mechanism: In NOMA, the SIC can eliminate the successive interference caused by spectrum multiplexing. According to the SIC decoding mechanism, the priority demodulation at the receiver judges the decoding order by the received power. The user with the larger received power has a higher decoding priority, which is applicable to both the uplink and the downlink in the NOMA system. For the uplink NOMA system, when the transmitter performance of each user is same, the user transmits with the better channel state has the higher decoding priority [36]. In the proposed system model, $I_{u,k}^{B,in}$, $I_{u,k}^{B,out}$, and $I_{u,k}^{SB}$ all should be considered as part of the channel state. Here, we provide the following theorem.

Theorem 1: In the uplink terrestrial-satellite multiple-cells NOMA networks, for $\forall u1, u2 \in M_k, k\in\mathbb{K}$, if the signal of $u1$ can be decoded and successfully removed from signal of $u2$ by the SIC, the corresponding channel coefficients satisfy:

$$|h_{u1,k}^B|^2 \ge |h_{u2,k}^B|^2. \tag{11}$$

Proof: The received power of BS k from $u1$ and $u2$ are respectively:

$$\begin{aligned} receive_{u1} &= |h_{u1,k}^B|^2(p_{u1,k}+p_{u2,k}) + I_{u1,k}^{B,out} + I_{u1,k}^{SB} + \sigma^2, \\ receive_{u2} &= |h_{u2,k}^B|^2(p_{u2,k}+p_{u1,k}) + I_{u2,k}^{B,out} + I_{u2,k}^{SB} + \sigma^2, \end{aligned} \tag{12}$$

where $I_{u1,k}^{B,out} = I_{u2,k}^{B,out} = \sum_{i\in\mathbb{K}\setminus\{k\}}\sum_{j\in M_i} |h_{j,i}^B|^2 p_{j,i}$ and $I_{u1,k}^{SB} = I_{u2,k}^{SB} = \sum_{j\in M_{K+1}} |h_{j,k}^B|^2 p_{j,K+1}$. According to the analysis above, if the signal of $u1$ is successfully decoded, $receive_{u1} \ge receive_{u2}$ is satisfied. Thus, $|h_{u1,k}^B|^2 \ge |h_{u2,k}^B|^2$ is obtained.

The proof is completed. ■

Assume that the channel coefficients of UEs with the terrestrial BS k are sorted as

$$Q(M_k) \triangleq |h_{1,k}^B|^2 \ge |h_{2,k}^B|^2 \ge \cdots \ge |h_{U,k}^B|^2, \quad \forall k\in K. \tag{13}$$

Let S_u denote the set $\{1,2,\cdots,u\}$, thus the SINR of BS k from UE u can be re-written as

$$\gamma_{u,k}^B = \frac{|h_{u,k}^B|^2 p_{u,k}}{|h_{u,k}^B|^2 \sum_{j\in M_k\setminus S_u} p_{j,k} + I_{u,k}^{B,out} + I_{u,k}^{SB} + \sigma^2}. \tag{14}$$

B. Problem Formulation

For the terrestrial UEs, the high achieved transmit rate is expected, which leads to a high transmit power and has a positive effect on the system performance. On the other hand, the cross-tier interference can affect QoS of the satellite UEs, which plays a negative role for the user communication [37]. Therefore, we construct the terrestrial UE's utility function which consists of the achieved rate and the cross-tier interference in the following.

$$U_{u,k}^{B} = \sum_{u \in M_k} \left(r_{u,k}^{B} - \omega |h_u^S|^2 p_{u,k} \right), \tag{15}$$

where ω denotes the interference pricing factor. From equation (15), the achieve rate has a positive effect on the utility function, while the cross-tier interference plays a negative role on it. Let U_k denote the achieved utility of BS k. Thus, the achieved system utility is

$$\mathcal{U} = \sum_{k \in \mathbb{K}} \sum_{u \in M_k} U_{u,k}^{B} = \sum_{k \in \mathbb{K}} U_k. \tag{16}$$

Thus, the resource allocation problem with related constraints for the uplink NOMA terrestrial-satellite networks is formulated as

$$\begin{aligned}
&\max_{\{\mathbb{X},\beta,\mathbb{P}\}} \sum_{k \in \mathbb{K}} U_k \\
&\text{s.t. } C1: \ Q(M_k), \forall k \in \mathbb{K} \cup \{K+1\}, (a) \\
&\quad C2: \ x_{u,k} \in \{0,1\}, \quad \forall k \in \mathbb{K} \cup \{K+1\}, \ \forall u \in \mathbb{U}, (b) \\
&\quad C3: \ \sum_{i \in \mathbb{K} \cup \{K+1\}} x_{u,i} = 1, \quad \forall u \in \mathbb{U}, (c) \\
&\quad C4: \ p_{u,k} \in [0, P_{\max}], \quad \forall u \in \mathbb{U}, \ \forall k \in \mathbb{K} \cup \{K+1\}, (d) \\
&\quad C5: \ r_{u,k}^{B} > r_u, \quad \forall k \in \mathbb{K}, \ \forall u \in \mathbb{U}, (e) \\
&\quad C6: \ \beta \in (0,1), (f) \\
&\quad C7: \ \sum_{j \in M_k} (1 - g_{j,k}) r_{j,k}^{B} < R_{k,s}, \quad \forall k \in \mathbb{K}. (g)
\end{aligned} \tag{17}$$

where $\mathbb{X}$, β, and $\mathbb{P}$ are the user association indicators, bandwidth assignment indicator, and the power allocation indicators, respectively. Constraint (17a) denotes the decoding order of cell k with the AP-UE association matrix $\mathbb{X}[x_{u,k}]_{U \times (K+1)}$. Constraint (17$b$) is the user association indicates, where $x_{u,k} = 1$ denotes the UE u served by BS k or satellite $K+1$, and $x_{u,k} = 0$, otherwise. Constraint (17c) denotes that a UE can only access one access point (AP) in each time slot. The power constraint is with (17d). Constraint (17e) guarantees the user's QoS. Constraint (17f) restricts the value range of the backhaul bandwidth factor. Constraint (17g) denotes the achieved sum rate of cell k should be less than its backhaul link rate.

The optimization problem (17) is a mixed-integer nonlinear programming problem, that is highly non-convex and has NP complexity [38], [39]. In the meanwhile, the update of user association strategy will lead to the change of user channel conditions, which makes it difficult to directly transform the optimization problem (17) into the convex one [21]. Therefore, the problem (17) is divided into three stages so as to solve the problem more efficiently.

III. Three-Stages Resource Allocation Method

The original optimization (17) is decoupled into AP-UE association, bandwidth assignment, and power allocation sub-problems in this section. Firstly, assuming that the UEs' power and bandwidth ratio is fixed, an AP-UE association scheme based on the caching state and preference relation is proposed. Then, the bandwidth allocation indicator is derived. According to the obtained $\mathbb{X}$ and β, we further focus on the power allocation sub-problem and propose an iterative algorithm to find the power solutions. The detailed description of solving the three sub-problems is given as follows.

A. AP-UE Association Method

The AP-UE association sub-problem is

$$\begin{aligned}
&\max_{\{\mathbb{X}\}} \sum_{k \in \mathbb{K}} U_k \\
&\text{s.t. } (17a), \ (17b), \ (17c).
\end{aligned} \tag{18}$$

In AP-UE association optimization sub-problem (18), the QoS of UE and backhaul link constraint is ignored to expand the range of user swapping to ensure the global of the optimized solutions. Here, an enhanced-caching, preference relation, and swapping based algorithm is proposed. The detailed description is as follows.

1) **Preparation process**. The satellite UEs are chosen by the channel coefficient ratio $\rho_u = \frac{|h_u^S|^2}{|h_u^B|^2}$, where $h_u^B = \{h_{u,1}^B, h_{u,2}^B, \ldots, h_{u,K}^B\}$. We sort the ρ_u in descending order, and choose the first M_{K+1} UEs served by satellite. The remaining UEs randomly access the BS according to their preference list $\{\mathrm{Pr}\,e\_UE_u\}_{(U-M_{K+1}) \times K}$ with the channel coefficient order. Let m_k^{UE} represent the position of BS k in $\{\mathrm{Pr}\,e\_UE_u\}$.

2) **Judge and Decide process**. Terrestrial UEs send the request signal in order by the $\{\mathrm{Pr}\,e\_UE_u\}$. For any $k1, k2 \in \mathbb{K}, k1 \neq k2$, the judge and decide rule is

$$\begin{aligned}
M_{k1\,u} &\succ M_{k2} \\
&\Leftrightarrow U_{u,k2}^{B}(\{M_{k1}, M_{k2}\}) \\
&< U_{u,k1}^{B}(\{M_{k1} \cup \{u\}, M_{k2} \backslash \{u\}\}).
\end{aligned} \tag{19}$$

The (19) indicates that UE u prefers BS $k1$ to $k2$ only if u can achieve a higher utility in BS $k1$ than in BS $k2$. For fully utilizing caching resources, the UEs prefer to access the BS that has cached the content they need. However, due to the inverse growth of channel quality and communication distance, the additional benefits brought by caching may not compensate for the high pathloss. Here, we introduce a weight α. Thus, for $g_{u,k} = 1$, the judge function is considered as follows.

$$V_{u,z} = g_{u,k} (1 + \gamma_{u,k}^{B})^{\alpha(1-\beta)} \Bigg/ \frac{(1 + \gamma_{u,z}^{B})^{\alpha(1-\beta)}}{(1 + \gamma_{z,s})^{\frac{(1-\alpha)\beta}{|\mathrm{M_z}|\mathrm{K}}}}, \quad \forall z \in \mathbb{Z}, \tag{20}$$

where α is the weight of fronthaul link and $\mathbb{Z} = \{z | m_z^{UE} < m_k^{UE}, \forall z \in \mathbb{K}\}$. If $V_{u,z} \geq 1$ is true for $\forall z \in \mathbb{Z}$, it is considered that the revenue of caching can offset the high pathloss caused by the communication distance, and UE u is served by BS z.

If $0 < V_{u,z} < \mathbb{Z}$ is true for $\exists z \in \mathbb{Z}$, the BS z can achieve higher revenue than BS k, and UE u chooses the BS z with the smallest $V_{u,z}$. Let A_u represent the actions of user u, the above can be summarized as (21), shown at the bottom of the page.

3) **Swap Matching process**. For any $k1, k2 \in \mathbb{K}, k1 \neq k2$ and $u1, u2 \in \mathbb{U}, U1 \neq U2$ with $x_{u1,k1} = 1, x_{u2,k2} = 1$, the swapping matching is described as follows.

$$\begin{aligned}\{M\}_{u1}^{u2} = &\{M\}\backslash\{M_{k1}, M_{k2}\} \\ &\cup \{M_{k1}\backslash\{u1\} \cup \{u2\}\} \\ &\cup \{M_{k2}\backslash\{u2\} \cup \{u1\}\}.\end{aligned} \tag{22}$$

Thus, the swapping rules can be defined as

$$\begin{aligned}\{M\}_{u1(u1,u2)}^{u2} &\succ \{M\} \\ &\Leftrightarrow \sum_{k\in\mathbb{K}} U_k(\{M\}) < \sum_{k\in\mathbb{K}} U_k(\{M\}_{u1}^{u2}).\end{aligned} \tag{23}$$

The (23) indicates that matching $\{M\}$ is updated to $\{M\}_{u1}^{u2}$ only if matching $\{M\}_{u1}^{u2}$ can achieve a higher system utility than matching $\{M\}$.

4) **End of the algorithm**. All the terrestrial UEs update the AP-UE association matrix $\mathbb{X}$ based on the **Judge and Decide process** and **Swap Matching process** until convergence.

In the Judge and Decide process, the user utility is considered with formula (19) to reduce complexity. The judge is finished when no UE intends to select other BSs. Then in the Swap Matching process, two UEs in the different cells are randomly selected and judged by system utility with formula (22) at each iteration, thus the optimization solution of the AP-UE association can be obtained.

B. Bandwidth Assignment

By original optimization problem (17), the bandwidth allocation sub-problem is

$$\begin{aligned}&\max_{\{\beta\}} \sum_{k\in\mathbb{K}} U_k \\ &\text{s.t. } C1' : Q(M_k^*), \quad \forall k \in \mathbb{K} \cup \{K+1\}, (a') \\ &\qquad (17f),\ (17g),\end{aligned} \tag{24}$$

where $Q(M_k^*)$ denotes the decoding sequence of cell k with the AP-UE association matrix $\mathbb{X}^*[x_{u,k}^*]$. The closed-form expression of the bandwidth allocation optimization sub-problem (24) is defined in the following.

Definition 1: In the bandwidth allocation optimization sub-problem (24), the optimal value β can be obtained as $\max_k LB_k$. For $\forall k \in \mathbb{K}$, the LB_k is as (25), shown at the bottom of the page.

Proof: The problem (24) can be formulated by condition $(17f)$ and $(17g)$. According to the $(17g)$, for $k \in \mathbb{K}$, we can derive the (26), shown at the bottom of the page. Thus, the optimization sub-problem (24) can be transformed into

$$\begin{aligned}&\max_{\{\beta\}} \sum_{k\in\mathbb{K}} U_k \\ &\text{s.t. } \max_k LB_k \leq \beta < 1, \quad \forall u \in \mathbb{U},\ k \in \mathbb{K}.\end{aligned} \tag{27}$$

From (27), the utility function is a monotonically decreasing function to β, so the optimal value β^* can be obtained at the lower bound. ■

C. Power Allocation

By (17), the power allocation sub-optimization problem can be written as

$$\begin{aligned}&\max_{\{\mathbb{P}\}} \sum_{i\in\mathbb{K}} U_k \\ &\text{s.t. } (24a'),\ (17d),\ (17e),\end{aligned} \tag{28}$$

$$A_u = \begin{cases} x_{u,k} = 1, & \text{if } g_{u,k} = 1, \text{ and } V_{u,z} \geq 1, \forall z \in \mathbb{Z}, \forall k \in \mathbb{K}, \\ \sum_{z\in\mathbb{Z}} x_{u,z} = 1, & \text{if } g_{u,k} = 1, \text{ and } 0 < V_{u,z} < 1, \exists z \in \mathbb{Z}, \forall k \in \mathbb{K}, \\ \text{judge and swap by (19)}, & \text{if } g_{u,k} = 0, \forall k \in \mathbb{K}. \end{cases} \tag{21}$$

$$LB_k = \frac{\sum_{j\in M_k^*}(1-g_{j,k})\log_2(1+\gamma_{j,k}^B)}{\frac{|M_k^*| - \sum_{j\in M_k^*} g_{j,k}}{|M_k^*|}\frac{1}{K}\log_2(1+\gamma_{k,o}^B) + \sum_{j\in M_k^*}(1-g_{j,k})\log_2(1+\gamma_{j,k}^B)}, \forall k \in \mathbb{K}. \tag{25}$$

$$\begin{aligned}&\sum_{j\in M_k^*}(1-g_{j,k})(1-\beta)B\log_2(1+\gamma_{j,k}^B) \\ &\quad\leq \frac{|M_k^*| - \sum_{j\in M_k^*} g_{j,k}}{|M_k^*|}\beta\frac{B}{K}\log_2(1+\gamma_{k,s}) \\ &\Rightarrow \beta \geq \frac{\sum_{j\in M_k^*}(1-g_{j,k})\log_2(1+\gamma_{j,k}^B)}{\frac{|M_k^*| - \sum_{j\in M_k^*} g_{j,k}}{|M_k^*|}\frac{1}{K}\log_2(1+\gamma_{k,s}) + \sum_{j\in M_k^*}(1-g_{j,k})\log_2(1+\gamma_{j,k}^B)} = LB_k \Rightarrow \beta \geq \max_k LB_k.\end{aligned} \tag{26}$$

which is non-convex because of the non-convex objective function $\sum_{k\in\mathbb{K}}\sum_{u\in M_k}\left(r^B_{u,k}-\omega|h^S_u|^2p_{u,k}\right)$ to $p_{u,k}$. Expand the objective function as (29), shown at the bottom of the page. The second term of objective function (29) is non-convex and needs to be convexly transformed. The successive convex approximation approach can overcome such the non-convex problem with good convergence and satisfying the KKT condition [40], [41]. According to the Taylor series expansion, the logarithmic approximation is obtained. For $\forall x^j>0, j\in[1,n]$, there exists $x^i_0>0$ which satisfies the following formula:

$$\begin{aligned}&-\sum_{i\in[1,n]}\log f^i(x^1,\cdots,x^j,\cdots,x^n)\\&\geq-\sum_{i\in[1,n]}\log f^i(x^1_0,\cdots,x^j_0,\cdots,x^n_0)\\&\quad-\sum_{j\in[1,n]}(x^j-x^j_0)\sum_{i\in[1,n]}\frac{{f^i_{x^j}}'(x^1_0,\cdots,x^j_0,\cdots,x^n_0)}{f^i(x^1_0,\cdots,x^j_0,\cdots,x^n_0)}.\end{aligned}\tag{30}$$

The inequality (30) provides the approximated upper bound of the logarithmic function [42], and it converges at $x^i=x^i_0$. Let

$$\begin{aligned}-\Phi=&-\sum_{k\in\mathbb{K}}\sum_{u\in M^*_k}\log_2(|h^B_{u,k}|^2\sum_{j\in M^*_k\backslash S_u}p_{j,k}+I^{B,out}_{u,k}\\&+I^{SB}_{u,k}+\sigma^2).\end{aligned}\tag{31}$$

We give the following definition.

Definition 2: The non-convex term $-\Phi$ of (31) can obtain the lower bound at $-\tilde{\Phi}$ and it converges at local point $p_{u,k}=p_{u,k}[l]$, where

$$\begin{aligned}\tilde{\Phi}=&\sum_{u\in M^*_k}\log_2(I^{B,in}_{u,k}[l]+I^{B,out}_{u,k}+I^{SB}_{u,k}+\sigma^2)\\&+\sum_{i\in\mathbb{K}\backslash\{k\}}\sum_{j\in M^*_i}\log_2(I^{B,in}_{j,i}+I^{B,out}_{j,i}[l]+I^{SB}_{j,i}+\sigma^2)\\&+\frac{1}{\ln 2}\sum_{u\in M^*_k}\sum_{j\in S_{u-1}}\frac{|h^B_{j,k}|^2(p_{u,k}-p_{u,k}[l])}{I^{B,in}_{j,k}[l]+I^{B,out}_{j,k}+I^{SB}_{j,k}+\sigma^2}\\&+\frac{1}{\ln 2}\sum_{u\in M^*_k}\sum_{i\in\backslash\{k\}}\sum_{j\in M^*_i}\frac{|h^B_{u,i}|^2(p_{u,k}-p_{u,k}[l])}{I^{B,in}_{j,i}+I^{B,out}_{j,i}[l]+I^{SB}_{j,i}+\sigma^2}.\end{aligned}\tag{32}$$

Algorithm 1 The Enhanced-Caching, Preference Relation, and Swapping Based AP-UE Association Algorithm

Initialize the UE preference list $\mathrm{Pr}\,e\_UE_u$ and optimal decoding order $Q(M_k)$ for $\forall u\in\mathbb{U},\forall k\in\mathbb{K}$.
Calculate and sort $\rho_u=\frac{|h^S_u|^2}{|h^B_u|^2}$ in descending order. Choose the first M_{K+1} UEs served by satellite.
Update $\mathbb{X}$ and terrestrial UE set $\mathbb{U}'$.
Judge and Decide Process
repeat
  for $\forall u\in\mathbb{U}'$ **do**
    if There exists the BS k with $g_{u,k}=1$ **then**
      Find set $\mathbb{Z}$ and calculate the $V_{u,z}$ by (20).
    end if
    Update $\mathbb{X}$ with $x_{u,k}$ by (21).
    Update $Q(M_k)$ by $\mathbb{X}$ for $\forall k\in\mathbb{K}$.
  end for
until Reach convergence
Swapping Process
repeat
  Select UEs $u1$, $u2$ in different cells randomly, and the new matching $\{M\}^{u2}_{u1}$ is obtained by (22).
  Calculate the new system utility of $\{M\}^{u2}_{u1}$.
  Update $\mathbb{X}$ with $x_{u,k}$ by (23).
until Reach convergence

The derivation process can be found in the appendix A.

By (32), the non-convex problem (28) can be transformed and formulated as (33), shown at the bottom of the page. Then, an iterative power allocation scheme is presented to solve the optimization problem (33). In the first iteration, the initial power $p_{u,k}[0]$ is provided and the power solution is obtained by interior point method. In the lth iteration, the calculated power value is treated as the initial value $p_{u,k}[l+1]$ of the next round. Continuing within the same loop iteration, the algorithm finally leads to convergence.

IV. Resource Optimization Algorithm Design

In this section, the corresponding algorithms are designed based on the discussion above. Also, we discuss the complexity analysis of the proposed algorithms.

A. Algorithm Design

By introducing the user association operation above, the Algorithm 1 shows the proposed AP-UE association algorithm for terrestrial-satellite HetNets. In Algorithm 1, the bandwidth and UE power are fixed. The UEs, BSs and satellite are

$$\begin{aligned}\max_{\{\mathbb{P}\}}\ &\{(1-\beta^*)B\sum_{k\in\mathbb{K}}\sum_{u\in M^*_k}\log_2(|h^B_{u,k}|^2p_{u,k}+|h^B_{u,k}|^2\sum_{t\in M^*_k\backslash S_u}p_{t,k}+I^{B,out}_{u,k}+I^{SB}_{u,k}+\sigma^2)\\&-(1-\beta^*)B\sum_{k\in\mathbb{K}}\sum_{u\in M^*_k}\log_2(|h^B_{u,k}|^2\sum_{t\in M^*_k\backslash S_u}p_{t,k}+I^{B,out}_{u,k}+I^{SB}_{u,k}+\sigma^2)-\omega\sum_{k\in\mathbb{K}}\sum_{u\in M^*_k}|h^S_u|^2p_{u,k}\}.\end{aligned}\tag{29}$$

$$\begin{aligned}\max_{\{\mathbb{P}\}}\ &\{(1-\beta^*)B\sum_{k\in\mathbb{K}}\sum_{u\in M^*_k}\log_2(|h^B_{u,k}|^2p_{u,k}+|h^B_{u,k}|^2\sum_{t\in M^*_k\backslash S_u}p_{t,k}+I^{B,out}_{u,k}+I^{SB}_{u,k}+\sigma^2)\\&-(1-\beta^*)B\tilde{\Phi}-\omega\sum_{k\in\mathbb{K}}\sum_{u\in M^*_k}|h^S_u|^2p_{u,k}\}\\&\text{s.t. }(24a'),\ (17d),\ (17e).\end{aligned}\tag{33}$$

Algorithm 2 A Three-Stages Resource Allocation Algorithm

Initialize $\mathbb{X}$, $\mathbb{P}$, β. Initialize the maximum tolerance $\varepsilon_{\max}$, and $l_{\max}$; Set $l = 0$.
AP-UE Association
Solve $\mathbb{X}^*$ with $x_{u,k}$ by **Algorithm 1**.
Update $Q(M_k^*)$ by $\mathbb{X}^*$ for $\forall k \in \mathbb{K}$.
Bandwidth Allocation
Calculate and solve $\beta^* = \max_k LB_k$ by (25).
Power Allocation
repeat
  for $\forall u \in \mathbb{U}, \forall k \in \mathbb{K}$ **do**
    Calculate and update $\mathbb{P}$ with $p_{u,k}$ by solving convex problem (33).
  end for
  $p_{u,k}[l+1] = p_{u,k}$, $l = l + 1$;
until $\left| \sum_{k\in\mathbb{K}} U_k[l] - \sum_{k\in\mathbb{K}} U_k[l-1] \right| < \varepsilon_{\max}$ or $l = l_{\max}$

performed as a many-to-many two-side matching. The satellite UEs are selected by the channel coefficient ratio and terrestrial UEs access the BS with higher utility of UE. In particular, the cached UEs determines the served BSs by calculating the value of constructed balance function. Then, the swapping matching is used to improve the quality of solutions by maximizing the system utility. Accordingly, a three-stages resource allocation algorithm is designed in Algorithm 2, where the AP-UE association solution $\mathbb{X}$ and bandwidth allocation coefficient β are used as the input of the power allocation sub-problem. The non-convex optimization problem is transformed into a convex problem by Taylor expansion, then the optimized power solution $\mathbb{P}$ can be obtained by iteration.

B. Complexity Analysis

We investigate the complexity analysis of the proposed AP-UE association, bandwidth assignment, power allocation algorithms in this subsection. In Algorithm 1, suppose that the iteration numbers for Judge and Decide Process and Swapping Process for convergence are I_1 and I_2, respectively. The complexity of solving user utility of each UE is U in each iteration of Judge and Decide Process. Hence, the complexity of Algorithm 1 is $O(I_1 \times U + I_2)$. In Algorithm 2, the worst-case situation by successive convex approximation is $l_{\max}$. At each iteration of power allocation algorithm in Algorithm 2, the calculation of (33) entails UK operations. The complexity for solving the power optimization sub-problem is $O(l_{\max} \times UK)$. Accordingly, the complexity of Algorithm 2 is $O(I_1 \times U + I_2 + l_{\max} \times UK + 1)$.

V. Simulation Results

The simulation experiments are discussed to verify the efficiency of the proposed algorithms. The parameters are set as follows. The altitude of the satellite and the radius of BSs are set as 1000 km, 50 m. The maximum transmit power of each UE is $P_u^{\max} = 23$ dBm. The transmit of each BS is set as 43 dBm. Assume that the total system bandwidth of terrestrial-satellite HetNets is $B = 20$ MHz for C-band, and the AWGN power $\sigma^2 = -174$ dBm/Hz [43]. The weight in the proposed AP-UE association scheme is set as $\alpha = 0.99$.

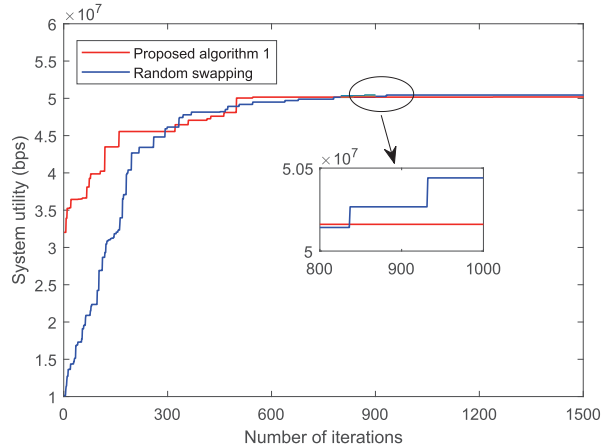

Fig. 2. The convergence of the proposed AP-UE association algorithm.

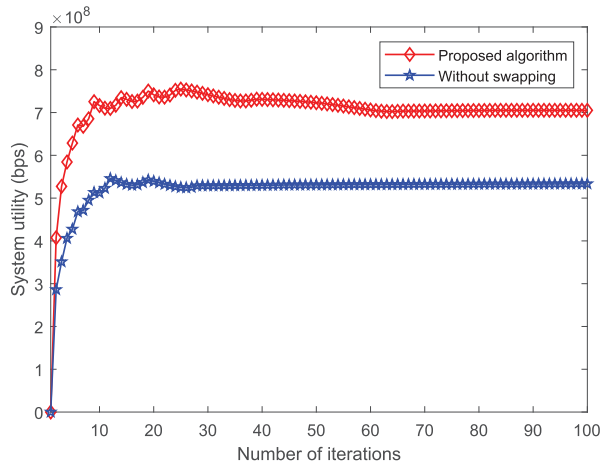

Fig. 3. The convergence of the proposed power allocation algorithm.

The number of UEs and terrestrial BSs are set as $U = 50$ and $K = 5$. The terrestrial link and satellite link are modeled as the Rayleigh fading and Rician fading [44], [45], respectively.

Fig. 2 shows the convergence comparison of different user association algorithms. The power of each UE and weight factor are set as $P_u = 23$ dBm and $\alpha = 0.99$, respectively. In Fig. 2, we can see that utility curves increase rapidly with both the proposed AP-UE association algorithm and the random swapping algorithm when the iteration starts, and become slower gradually until the algorithms converge. The proposed algorithm converges within 500 to 600 iterations, and the random swapping algorithm needs approximately 1000 iterations. It suggests the computational complexity is rather low in the proposed AP-UE association algorithm.

Fig. 3 shows the relationship between the utility convergence comparison of the proposed algorithm 2 by different AP-UE association schemes. It is obvious that the system utility finally converges to a stable value, which confirms the convergence of the successive convex approximation based power allocation algorithm. Fig. 3 further implies that the system utility by our proposed algorithm is higher than the scheme without swapping process.

Fig. 4 illustrates the system utility versus the number of UEs under different schemes. We compare the proposed scheme with the ideal backhaul (IBH) scheme, random power

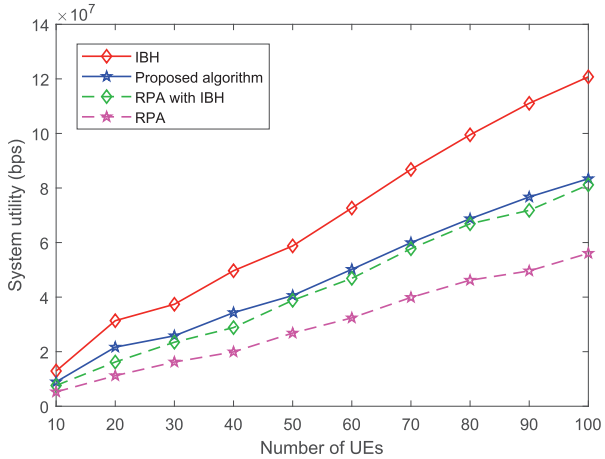

Fig. 4. The system utility versus the number of UEs with different schemes.

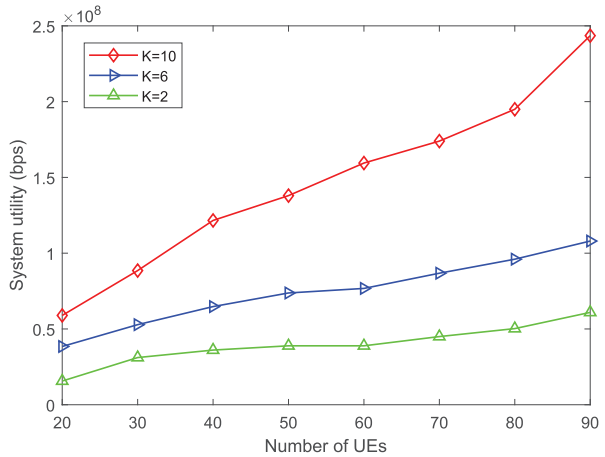

Fig. 5. The system utility versus the number of UEs with different K.

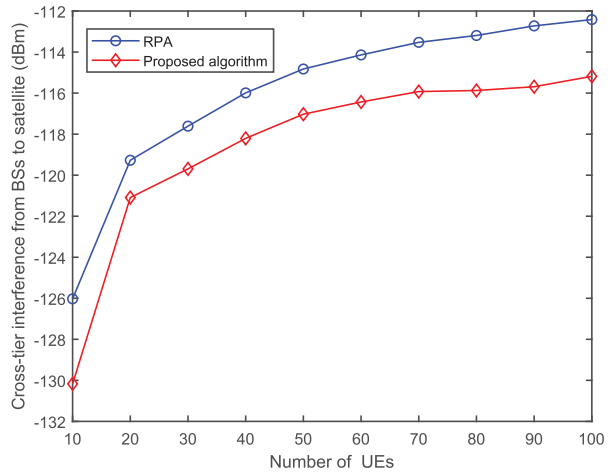

Fig. 6. The cross-tier interference from terrestrial BSs to satellite versus the number of UEs.

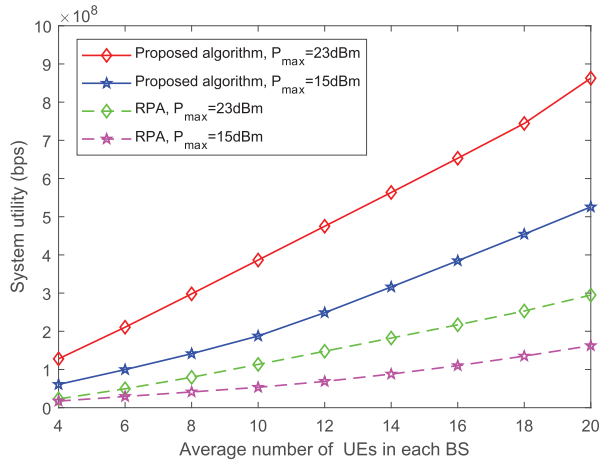

Fig. 7. The system utility versus the average number of UEs in each terrestrial BSs with different P_{max}.

allocation (RPA) scheme, and the PRA with IBH scheme. With the increase of UE number, the system utility of four schemes increases. Furthermore, it is observed that the system utility using the proposed scheme is close to the case with IBH scheme and has a higher system utility than the RPA scheme and the RPA with IBH scheme. Also, the system utility of RPA scheme with IBH is higher than the case with backhaul constraint. The reason is that in IBH scheme expands the feasible region of optimization problem, resulting in the increased system utility in terrestrial-satellite networks.

Fig. 5 describes the system utility performance versus the number of UEs when the number of BSs is set as 10, 6, and 2. It can be shown that the increase in the number of BSs brings the higher system utility. The reason is that when the number of the UES is fixed, with the increase of the number of terrestrial BSs, each terrestrial UE has more choices of candidate BSs, which results in the better performance.

Fig. 6 shows the cross-tier interference from terrestrial BSs to satellite versus different number of UEs. The RPA scheme is provided to compare the performance. In user association part, the proposed AP-UE association scheme is also applied in the RPA scheme. From the Fig. 6, it can be seen that as the rise of the number of UEs, the system utility increases. Moreover, the cross-tier interference caused by terrestrial BSs to satellite of our proposed algorithm is less than the RPA scheme, which is because that the cross-tier interference affects the system utility as a negative effect in the proposed model. Therefore, the UEs are unable to increase power blindly to obtain higher achieved transmit rate. The QoS of the satellite UEs can be guaranteed.

Fig. 7 depicts the system utility versus average number of UEs in each terrestrial BS as the proposed algorithm and RPA algorithm. The number of BSs is 5. From Fig. 7, it is obvious that the system utility gradually increases with the average number of UEs in each terrestrial BS rising. The higher maximum power of each UE will yield a high system utility. Moreover, the system utility of our proposed algorithm is significantly higher than the RPA scheme, and the performance improvement of system utility is more obvious as the rise of the UEs.

Fig. 8 shows the increase of the system utility as the number of terrestrial BSs increases when the maximum power of each UEs is set to 23 dBm, 20 dBm, and 15 dBm. In Fig. 8, the number of UEs is 50. It can be seen that the trend with different number of BSs is very similar to the average number of UEs in each terrestrial BS. The system utility increases as the maximum power of each UE increases. The reason is that the high maximum power expands the value range of the

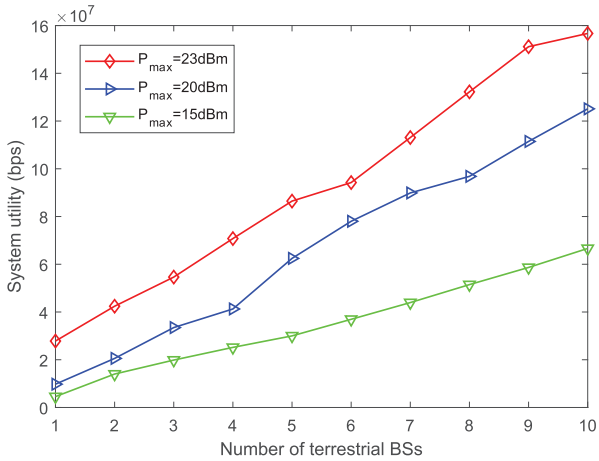

Fig. 8. The system utility versus the number of UEs with different P_{max}.

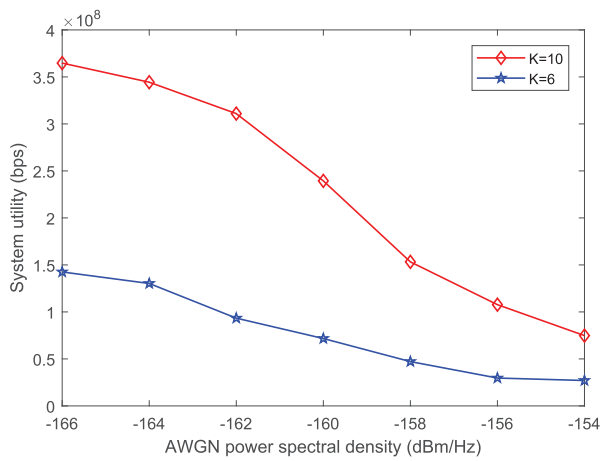

Fig. 9. The system utility versus the AWGN power spectral density with different K.

power optimization solutions, which can significantly increase system utility for the terrestrial-satellite networks.

Fig. 9 provides the curve of the system utility versus the AWGN power spectral density from -166 dBm to -154 dBm when the number of terrestrial BSs equals to 10 and 6. We set the number of UEs to 100 in this figure. From Fig. 9, with the increase of AWGN power spectral density, the system utility gradually decreases. For the same AWGN power spectral density, the more terrestrial BSs, the higher system utility can be obtained.

VI. Conclusion

This paper studied AP-UE association, bandwidth assignment, and power allocation problem in uplink caching based NOMA terrestrial-satellite HetNets, where the satellite provided backhaul link and UEs shared radio spectrum resources by access links with NOMA. Specifically, a utility function that consists of the achieved rate of terrestrial UEs and the cross-tier interference of satellite UEs was designed. Thus, the resource optimization problem was established by considering the UE's QoS and satellite backhaul constraint. Because of the non-convexity of the original optimization problem, we divided it into three stages. The first stage focused on the AP-UE association sub-problem. An enhanced-caching, preference relation, and swapping based algorithm was proposed. The second stage provided the derived closed-form expression of the bandwidth assignment coefficient. Moreover, the power allocation sub-problem was studied in the third stage, in which the non-convex power optimization problem was transformed through the successive convex approximation method and solved by an iterative power allocation scheme. Finally, a three-stages iterative resource optimization algorithm was designed to obtain the utility performance improvement. The simulation results verified the effectiveness of the proposed algorithms.

Appendix
Proof of the Definition 2

Decompose the expression (31) as

$$\Phi = \sum_{k\in\mathbb{K}}\sum_{u\in M_k^*}\log_2(|h_{u,k}^B|^2\sum_{j\in M_k^*\backslash S_u}p_{j,k}+I_{u,k}^{B,out}+I_{u,k}^{SB}+\sigma^2)=\Phi_1+\Phi_2, \tag{34}$$

where Φ_1 and Φ_2 are as (35) and (36), respectively.

$$\Phi_1 = \sum_{u\in M_k^*}\log_2(|h_{u,k}^B|^2\sum_{j\in M_k^*\backslash S_u}p_{j,k}+I_{u,k}^{B,out}+I_{u,k}^{SB}+\sigma^2), \tag{35}$$

$$\Phi_2 = \sum_{i\in\mathbb{K}\backslash\{k\}}\sum_{j\in M_i^*}\log_2(|h_{j,i}^B|^2\sum_{t\in M_i^*\backslash S_j}p_{t,i}+\sum_{m\in\mathbb{K}\backslash\{i\}}\sum_{t\in M_m^*}|h_{t,i}^B|^2p_{t,m}+I_{j,i}^{SB}+\sigma^2). \tag{36}$$

In (35), the target power $p_{u,k}$ only influence the successive interference term caused by NOMA. Based on the Theorem 1, for UE j and UE u with $j \geq u$ in cell k, the UE j can not receive the successive interference from UE u. Thus, based on the (30), the convex upper bound of Φ_1 can be simplified and derived into

$$\Phi_1 \leq \sum_{u\in M_k^*}\log_2(|h_{u,k}^B|^2\sum_{t\in M_k^*\backslash S_u}p_{t,k}[l]+I_{u,k}^{B,out}+I_{u,k}^{SB}+\sigma^2)+\frac{1}{\ln 2}\sum_{u\in M_k^*}D_{u,k}^1(p_{u,k}-p_{u,k}[l]), \tag{37}$$

where

$$D_{u,k}^1 = \sum_{j\in S_{u-1}}\frac{|h_{j,k}^B|^2}{|h_{j,k}^B|^2\sum_{t\in M_k^*\backslash S_j}p_{t,k}+I_{j,k}^{B,out}+I_{j,k}^{SB}+\sigma^2}. \tag{38}$$

Similarly, the target power $p_{u,k}$ only influence the cross-tier interference term in (34). The convex upper bound of Φ_2 is

$$\Phi_2 \leq \sum_{i\in\mathbb{K}\backslash\{k\}}\sum_{j\in M_i^*}\log_2(|h_{j,i}^B|^2\sum_{t\in M_i^*\backslash S_j}p_{t,i}+\sum_{m\in\mathbb{K}\backslash\{i\}}\sum_{t\in M_m^*}|h_{t,i}^B|^2p_{t,m}[l]+I_{j,i}^{SB}+\sigma^2)+\frac{1}{\ln 2}\sum_{u\in M_k^*}D_{u,k}^2(p_{u,k}-p_{u,k}[l]), \tag{39}$$

where $D_{u,k}^2$ is equation (40), as shown at the top of the next page.

$$D_{u,k}^2 = \frac{1}{\ln 2} \sum_{i \in \mathbb{K}\backslash\{k\}} \sum_{j \in M_i^*} \frac{|h_{u,i}^B|^2}{|h_{j,i}^B|^2 \sum\limits_{t \in M_i^* \backslash S_j} p_{t,i} + \sum\limits_{m \in \mathbb{K}\backslash\{i\}} \sum\limits_{t \in M_m^*} |h_{t,i}^B|^2 p_{t,m} + I_{j,i}^{SB} + \sigma^2}. \tag{40}$$

$$\begin{aligned} -\Phi \geq & -\sum_{u \in M_k^*} \log_2(|h_{u,k}^B|^2 \sum_{t \in M_k^* \backslash S_u} p_{t,k}[l] + I_{u,k}^{B,out} + I_{u,k}^{SB} + \sigma^2) \\ & - \sum_{i \in \mathbb{K}\backslash\{k\}} \sum_{j \in M_i^*} \log_2(|h_{j,i}^B|^2 \sum_{t \in M_i^* \backslash S_j} p_{t,i} + \sum_{m \in \mathbb{K}\backslash\{i\}} \sum_{t \in M_m^*} |h_{t,i}^B|^2 p_{t,m}[l] + I_{j,i}^{SB} + \sigma^2) \\ & - \frac{1}{\ln 2} \sum_{u \in M_k^*} D_{u,k}^1 (p_{u,k} - p_{u,k}[l]) - \frac{1}{\ln 2} \sum_{u \in M_k^*} D_{u,k}^2 (p_{u,k} - p_{u,k}[l]) = -\tilde{\Phi}. \end{aligned} \tag{41}$$

Based on the Taylor expansion, the lower bound of $-\Phi$ can be obtained as formula (41), as shown at the top of the page, which converges at $p_{u,k} = p_{u,k}[l]$.

The proof is completed.

REFERENCES

[1] G. Giambene, S. Kota, and P. Pillai, "Satellite-5G integration: A network perspective," *IEEE Netw.*, vol. 32, no. 5, pp. 25–31, Sep./Oct. 2018.

[2] O. Maraqa, A. S. Rajasekaran, S. Al-Ahmadi, H. Yanikomeroglu, and S. M. Sait, "A survey of rate-optimal power domain NOMA with enabling technologies of future wireless networks," *IEEE Commun. Surveys Tuts.*, vol. 22, no. 4, pp. 2192–2235, 4th Quart., 2020.

[3] S. Fu, J. Gao, and L. Zhao, "Collaborative multi-resource allocation in terrestrial-satellite network towards 6G," *IEEE Trans. Wireless Commun.*, vol. 20, no. 11, pp. 7057–7071, Nov. 2021.

[4] U. Gustavsson *et al.*, "Implementation challenges and opportunities in beyond-5G and 6G communication," *IEEE J. Microw.*, vol. 1, no. 1, pp. 86–100, Jan. 2021.

[5] W. Saad, M. Bennis, and M. Chen, "A vision of 6G wireless systems: Applications, trends, technologies, and open research problems," *IEEE Netw.*, vol. 34, no. 3, pp. 134–142, May/Jun. 2019.

[6] J. Du, C. Jiang, H. Zhang, Y. Ren, and M. Guizani, "Auction design and analysis for SDN-based traffic offloading in hybrid satellite-terrestrial networks," *IEEE J. Sel. Areas Commun.*, vol. 36, no. 10, pp. 2202–2217, Oct. 2018.

[7] E. Lagunas, S. K. Sharma, S. Maleki, S. Chatzinotas, and B. Ottersten, "Resource allocation for cognitive satellite communications with incumbent terrestrial networks," *IEEE Trans. Cognit. Commun. Netw.*, vol. 1, no. 3, pp. 305–317, Sep. 2015.

[8] Y. Li, H. Zhang, and K. Long, "Joint resource, trajectory, and artificial noise optimization in secure driven 3-D UAVs with NOMA and imperfect CSI," *IEEE J. Sel. Areas Commun.*, vol. 39, no. 11, pp. 3363–3377, Nov. 2021.

[9] W. Bao, H. Chen, Y. Li, and B. Vucetic, "Joint rate control and power allocation for non-orthogonal multiple access systems," *IEEE J. Sel. Areas Commun.*, vol. 35, no. 12, pp. 2798–2811, Dec. 2017.

[10] L. Liu, S. Zhang, and R. Zhang, "Multi-beam UAV communication in cellular uplink: Cooperative interference cancellation and sum-rate maximization," *IEEE Trans. Wireless Commun.*, vol. 18, no. 10, pp. 4679–4691, Oct. 2019.

[11] H. Zhang *et al.*, "Energy efficient dynamic resource optimization in NOMA system," *IEEE Trans. Wireless Commun.*, vol. 17, no. 9, pp. 5671–5683, Sep. 2018.

[12] A. I. Perez-Neira, M. Caus, and M. A. Vazquez, "Non-orthogonal transmission techniques for multibeam satellite systems," *IEEE Commun. Mag.*, vol. 57, no. 12, pp. 58–63, Dec. 2019.

[13] I. Randrianantenaina, M. Kaneko, H. Dahrouj, H. ElSawy, and M.-S. Alouini, "Interference management in NOMA-based fog-radio access networks via scheduling and power allocation," *IEEE Trans. Commun.*, vol. 68, no. 8, pp. 5056–5071, Aug. 2020.

[14] I. Budhiraja, N. Kumar, and S. Tyagi, "Cross-layer interference management scheme for D2D mobile users using NOMA," *IEEE Syst. J.*, vol. 15, no. 2, pp. 3109–3120, Jun. 2021.

[15] A. Celik, M.-C. Tsai, R. M. Radaydeh, F. S. Al-Qahtani, and M.-S. Alouini, "Distributed cluster formation and power-bandwidth allocation for imperfect NOMA in DL-HetNets," *IEEE Trans. Commun.*, vol. 67, no. 2, pp. 1677–1692, Feb. 2019.

[16] A. J. Muhammed, Z. Ma, Z. Zhang, P. Fan, and E. G. Larsson, "Energy-efficient resource allocation for NOMA based small cell networks with wireless backhauls," *IEEE Trans. Commun.*, vol. 68, no. 6, pp. 3766–3781, Jun. 2020.

[17] L. Wang, Y. Wu, H. Zhang, S. Choi, and V. C. M. Leung, "Resource allocation for NOMA based space-terrestrial satellite networks," *IEEE Trans. Wireless Commun.*, vol. 20, no. 2, pp. 1065–1075, Feb. 2021.

[18] J. Chu, X. Chen, C. Zhong, and Z. Zhang, "Robust design for NOMA-based multibeam LEO satellite Internet of Things," *IEEE Internet Things J.*, vol. 8, no. 3, pp. 1959–1970, Feb. 2021.

[19] Z. Lin, M. Lin, J.-B. Wang, T. de Cola, and J. Wang, "Joint beamforming and power allocation for satellite-terrestrial integrated networks with non-orthogonal multiple access," *IEEE J. Sel. Areas Commun.*, vol. 13, no. 3, pp. 657–670, Jun. 2019.

[20] X. Zhu, C. Jiang, L. Kuang, N. Ge, and J. Lu, "Non-orthogonal multiple access based integrated terrestrial-satellite networks," *IEEE J. Sel. Areas Commun.*, vol. 35, no. 10, pp. 2253–2267, Oct. 2017.

[21] K. Wang, Y. Liu, Z. Ding, A. Nallanathan, and M. Peng, "User association and power allocation for multi-cell non-orthogonal multiple access networks," *IEEE Trans. Wireless Commun.*, vol. 18, no. 11, pp. 5284–5298, Nov. 2019.

[22] J. Jiao, Y. Sun, S. Wu, Y. Wang, and Q. Zhang, "Network utility maximization resource allocation for NOMA in satellite-based Internet of Things," *IEEE Internet Things J.*, vol. 7, no. 4, pp. 3230–3242, Apr. 2020.

[23] X. Wang, M. Chen, T. Taleb, A. Ksentini, and V. C. M. Leung, "Cache in the air: Exploiting content caching and delivery techniques for 5G systems," *IEEE Commun. Mag.*, vol. 52, no. 2, pp. 131–139, Feb. 2014.

[24] L. Li, G. Zhao, and R. S. Blum, "A survey of caching techniques in cellular networks: Research issues and challenges in content placement and delivery strategies," *IEEE Commun. Surveys Tuts.*, vol. 20, no. 3, pp. 1710–1732, 3rd Quart., 2018.

[25] Z. Song, Y. Hao, Y. Liu, and X. Sun, "Energy-efficient multiaccess edge computing for terrestrial-satellite Internet of Things," *IEEE Internet Things J.*, vol. 8, no. 18, pp. 14202–14218, Sep. 2021.

[26] S. Fu, J. Gao, and L. Zhao, "Integrated resource management for terrestrial-satellite systems," *IEEE Trans. Veh. Technol.*, vol. 69, no. 3, pp. 3256–3266, Mar. 2020.

[27] J. Li, K. Xue, D. S. L. Wei, J. Liu, and Y. Zhang, "Energy efficiency and traffic offloading optimization in integrated satellite/terrestrial radio access networks," *IEEE Trans. Wireless Commun.*, vol. 19, no. 4, pp. 2367–2381, Apr. 2020.

[28] H. Zhang, H. Zhang, W. Liu, K. Long, J. Dong, and V. C. M. Leung, "Energy efficient user clustering, hybrid precoding and power optimization in terahertz MIMO-NOMA systems," *IEEE J. Sel. Areas Commun.*, vol. 38, no. 9, pp. 2074–2085, Sep. 2020.

[29] Y. Fu, W. Wen, Z. Zhao, T. Q. S. Quek, S. Jin, and F.-C. Zheng, "Dynamic power control for NOMA transmissions in wireless caching networks," *IEEE Wireless Commun. Lett.*, vol. 8, no. 5, pp. 1485–1488, Oct. 2019.

[30] Z. Yang, Y. Liu, Y. Chen, and N. Al-Dhahir, "Cache-aided NOMA mobile edge computing: A reinforcement learning approach," *IEEE Trans. Wireless Commun.*, vol. 19, no. 10, pp. 6899–6915, Oct. 2020.

[31] Z. Ding, P. Fan, G. K. Karagiannidis, R. Schober, and H. V. Poor, "NOMA assisted wireless caching: Strategies and performance analysis," *IEEE Trans. Commun.*, vol. 66, no. 10, pp. 4854–4876, Oct. 2018.

[32] L. Qi, M. Peng, Y. Liu, and S. Yan, "Advanced user association in non-orthogonal multiple access-based fog radio access networks," *IEEE Trans. Commun.*, vol. 67, no. 12, pp. 8408–8421, Dec. 2019.

[33] Y. Zhang, H. Zhang, H. Zhou, and W. Li, "Interference cooperation based resource allocation in NOMA terrestrial-satellite networks," in *Proc. IEEE GLOBECOM*, Madrid, Spain, Dec. 2021, pp. 1–5.
[34] H. Zhou, X. Chen, S. He, J. Chen, and J. Wu, "DRAIM: A novel delay-constraint and reverse auction-based incentive mechanism for WiFi offloading," *IEEE J. Sel. Areas Commun.*, vol. 38, no. 4, pp. 711–722, Apr. 2020.
[35] Y. Yang, S. Zhang, J. P. Lie, and R. Zhang, "Flexible multi-group single-carrier modulation: Subcarrier mapping and power allocation optimization," *IEEE Trans. Commun.*, vol. 67, no. 3, pp. 2002–2014, Mar. 2019.
[36] A. Akbar, S. Jangsher, and F. A. Bhatti, "NOMA and 5G emerging technologies: A survey on issues and solution techniques," *Comput. Netw.*, vol. 190, May 2021, Art. no. 107950.
[37] Y. Tang, P. Yang, W. Wu, J. W. Mark, and X. Shen, "Interference mitigation via cross-tier cooperation in heterogeneous cloud radio access networks," *IEEE Trans. Cognit. Commun. Netw.*, vol. 6, no. 1, pp. 201–213, Mar. 2020.
[38] M. Garey and D. S. Johnson, *Computers and Tntractability*, vol. 29. New York, NY, USA: Freeman, 2002.
[39] Z. Han, *Game Theory in Wireless and Tommunication Networks: Theory, Models, and Applications*. Cambridge, U.K.: Cambridge Univ. Press, 2012.
[40] H. Zhang, J. Zhang, and K. Long, "Energy efficiency optimization for NOMA UAV network with imperfect CSI," *IEEE J. Sel. Areas Commun.*, vol. 38, no. 12, pp. 2798–2809, Dec. 2020.
[41] W.-S. Lai, T.-H. Chang, and T.-S. Lee, "Joint power and admission control for spectral and energy efficiency maximization in heterogeneous OFDMA networks," *IEEE Trans. Wireless Commun.*, vol. 15, no. 5, pp. 3531–3547, May 2016.
[42] S. Boyd and L. Vandenberghe, *Convex Optimization*. Cambridge, U.K.: Cambridge Univ. Press, 2004.
[43] H. Zhang, M. Feng, K. Long, G. K. Karagiannidis, V. C. M. Leung, and H. V. Poor, "Energy efficient resource management in SWIPT enabled heterogeneous networks with NOMA," *IEEE Trans. Wireless Commun.*, vol. 19, no. 2, pp. 835–845, Feb. 2020.
[44] B. Di, H. Zhang, L. Song, Y. Li, and G. Y. Li, "Ultra-dense LEO: Integrating terrestrial-satellite networks into 5G and beyond for data offloading," *IEEE Trans. Wireless Commun.*, vol. 18, no. 1, pp. 47–62, Jan. 2019.
[45] E. Lutz, D. Cygan, M. Dippold, F. Dolainsky, and W. Papke, "The land mobile satellite communication channel-recording, statistics, and channel model," *IEEE Trans. Veh. Technol.*, vol. 40, no. 2, pp. 375–386, May 1991.

Yaomin Zhang received the M.S. degree from the Beijing University of Chemical Technology, Beijing, China, in 2019. She is currently pursuing the Ph.D. degree with the University of Science and Technology Beijing, China. Her research interests include 6G networks, fog computing, and resource allocation in wireless communication networks.

Haijun Zhang (Senior Member, IEEE) was a Post-Doctoral Research Fellow with the Department of Electrical and Computer Engineering, The University of British Columbia (UBC), Canada. He is currently a Full Professor and an Associate Dean at the University of Science and Technology Beijing, China. He received the IEEE CSIM Technical Committee Best Journal Paper Award in 2018, the IEEE ComSoc Young Author Best Paper Award in 2017, and the IEEE ComSoc Asia–Pacific Best Young Researcher Award in 2019. He serves/served as the Track Co-Chair for WCNC 2020, the Symposium Chair for Globecom'19, the TPC Co-Chair for INFOCOM 2018 Workshop on Integrating Edge Computing, Caching, and Offloading in Next Generation Networks, and the General Co-Chair for GameNets'16. He serves as an Editor for IEEE TRANSACTIONS ON COMMUNICATIONS, and IEEE TRANSACTIONS ON NETWORK SCIENCE AND ENGINEERING.

Huan Zhou (Member, IEEE) received the Ph.D. degree from the Department of Control Science and Engineering, Zhejiang University, in 2014. He was a Visiting Scholar with Temple University from November 2012 to May 2013 and a CSC supported Post-Doctoral Fellow at The University of British Columbia from November 2016 to November 2017. He is currently a Full Professor with the College of Computer and Information Technology, China Three Gorges University. He has published more than 50 research papers in some international journals and conferences, including IEEE JOURNAL ON SELECTED AREAS IN COMMUNICATIONS, IEEE TRANSACTIONS ON PARALLEL AND DISTRIBUTED SYSTEMS, and IEEE TRANSACTIONS ON VEHICULAR TECHNOLOGY. His research interests include mobile social networks, VANETs, opportunistic mobile networks, and mobile data offloading. He was a TPC Member of the IEEE WCSP'13'14, CCNC'14'15, ICNC'14'15, ANT'15'16, IEEE Globecom'17'18, and ICC'18'19. He received the Best Paper Award of I-SPAN 2014 and I-SPAN 2018. He was the Special Session Chair of the 3rd International Conference on Internet of Vehicles (IOV 2016). He was a Lead Guest Editor of *Pervasive and Mobile Computing*. He is currently serving as an Associate Editor of IEEE ACCESS and *EURASIP Journal on Wireless Communications and Networking*.

Keping Long (Senior Member, IEEE) received the M.S. and Ph.D. degrees from UESTC in 1995 and 1998, respectively. From July 2001 to November 2002, he was a Research Fellow with the ARC Special Research Centre for Ultra Broadband Information Networks (CUBIN), The University of Melbourne, Australia. He is currently a Professor and the Dean of the School of Computer and Communication Engineering (CCE), University of Science and Technology Beijing (USTB). He is/was a member of the Editorial Committee of *Sciences in China* (Series F) and *China Communications*. He is/was also a TPC and ISC Member of COIN, IEEE IWCN, ICON, and APOC, and the Organizing Co-Chair of IWCMC'06, the TPC Chair of COIN'05/'08, and the TPC Co-Chair of COIN'08/'10. He was awarded the National Science Fund Award for Distinguished Young Scholars of China in 2007 and selected as the Chang Jiang Scholars Program Professor of China in 2008.

George K. Karagiannidis (Fellow, IEEE) was born in Pithagorion, Samos, Greece. He received the University Diploma (five years) and Ph.D. degrees in electrical and computer engineering from the University of Patras in 1987 and 1999, respectively. From 2000 to 2004, he was a Senior Researcher at the Institute for Space Applications and Remote Sensing, National Observatory of Athens, Greece. In June 2004, he joined the Faculty of Aristotle University of Thessaloniki, Greece, where he is currently a Professor with the Electrical and Computer Engineering Department and the Head of the Wireless Communications and Information Processing (WCIP) Group. He is also a Honorary Professor at Southwest Jiaotong University, Chengdu, China. His research interests are in the broad area of digital communications systems and signal processing, with emphasis on wireless communications, optical wireless communications, wireless power transfer and applications, and communications and signal processing for biomedical engineering. He is one of the highly cited authors across all areas of electrical engineering, recognized by Clarivate Analytics as a Web-of-Science Highly Cited Researcher for the six consecutive years 2015 to 2020. He has been involved as the general chair, the technical program chair, and a member of technical program committees of several IEEE and non-IEEE conferences. In the past, he was an editor of several IEEE journals, and from 2012 to 2015, he was the Editor-in-Chief of IEEE COMMUNICATIONS LETTERS. Currently, he serves as an Associate Editor-in-Chief for IEEE OPEN JOURNAL OF THE COMMUNICATIONS SOCIETY.